



UNDERWATER OPTICAL COMMUNICATION

AUTHOR: AGUSTIN CASUSO CABARGA

SUPERVISOR: LUCIE HUDCOVÁ

6 MAY 2024

ASSIGNMENT

The project would involve the following tasks:

1. Obtaining and processing datasets for the global seabed profile (depth profile).
2. Finding datasets with surface temperature for each month of the year and calculating the depth temperature profile of the water medium.
3. Acquiring datasets for surface chlorophyll concentration and subsequently determining the depth profile of chlorophyll concentration. Additionally, exploring suitable models for determining the depth concentration of chlorophyll.
4. Calculating the specific attenuation of the water environment for a selected point, latitude, longitude, depth, and wavelength on Earth.
5. Computing the optical beam attenuation between two user-specified points.

The result should be a program that facilitates these calculations.

Abstract

Although a field as underwater optical communications can encompass different technological fields, in this bachelor thesis we will focus on underwater wireless communications, which, although underwater optical communications is dominated using cable, we can find multiple advantages, such as high transmission speed and wide transmission spectrum with minimal optical signal latency.

The main objective of this work is to develop a program to compute the attenuation of the optical beam between two user-specified points.

For this purpose, a MATLAB program has been developed, in which, first, the seabed profile is processed. Then, with the help of datasets, we will calculate the mean annual temperature at the water surface, as well as the surface chlorophyll. Once we have these values, we calculate the depth temperature profile and the depth profile of chlorophyll concentration. Then, we will be able to calculate the specific attenuation at a point with a given longitude, latitude, depth, and wavelength, and finally we will be able to compute the optical beam attenuation between two user-specified points.

Keywords

Underwater optical communication, chlorophyll-a, specific attenuation, optical beam attenuation.

Abstrakt

Ačkoli oblast podvodní optické komunikace může zahrnovat různá technologická pole, v této bakalářské práci se zaměříme na podvodní bezdrátovou komunikaci. I když v podvodní optické komunikaci dominuje použití kabelů, můžeme nalézt několik výhod, jako je vysoká přenosová rychlost a široké přenosové spektrum s minimální latencí optického signálu.

Hlavním cílem této práce je vyvinout program pro výpočet útlumu optického paprsku mezi dvěma uživatelem zadanými body.

Za tímto účelem byl vyvinut program MATLAB, ve kterém se nejprve zpracuje profil mořského dna. Poté s pomocí datových sad vypočítáme průměrnou roční teplotu na hladině vody a povrchový chlorofyl. Jakmile máme tyto hodnoty, vypočítáme hloubkový profil teploty a hloubkový profil koncentrace chlorofylu. Poté budeme schopni vypočítat specifický útlum v bodě s danou zeměpisnou délkou, šířkou, hloubkou a vlnovou délkou a nakonec budeme schopni vypočítat útlum optického paprsku mezi dvěma uživatelem zadanými body.

Klíčová slova

Podvodní optická komunikace, chlorofyl-a, specifický útlum, útlum optického paprsku.

Acknowledgement

To my parents, for always believing in me and giving me the wings that led me to discover this beautiful degree.

To my family, for their unconditional love and making me feel so cherished.

To my friends, for supporting me and always being there for me, in good times and bad.

CONTENTS

1. INTRODUCTION.....	8
1.1 STATE-OF-THE-ART	8
2. HOW WATER MEDIUM INTERACTS WITH OPTICAL BEAMS	11
2.1 SPECIFIC ATTENUATION.....	11
2.2 CHLOROPHYLL PROFILE.....	13
2.3 TEMPERATURE PROFILE.....	15
2.4 DEPTH DEPENDENCE.....	16
2.5 LIMITATIONS	17
3. MATLAB PROGRAM	18
3.1 INPUT DATA	18
3.2 USER-SPECIFIED POINTS	19
3.3 DEPTH TEMPERATURE PROFILE OF THE WATER MEDIUM.....	21
3.4 DEPTH CONCENTRATION OF CHLOROPHYLL.....	22
3.5 CALCULATION BETWEEN THE USER-SPECIFIED POINTS.....	23
3.6 CALCULATION OF THE SPECIFIC ATTENUATION	25
3.7 COMPUTING THE OPTICAL BEAM ATTENUATION	25
4. RESULTS.....	27
5. CONCLUSION.....	33

INTRODUCTION

In this bachelor thesis we enter in the field of submarine optical communications, a field that encompasses several technological areas. However, our focus is on wireless submarine communications, where optics play a crucial role. Although submarine optical communications are often dominated by cables, we explore the many advantages of wireless, such as high transmission speed and wide transmission spectrum with minimal optical signal latency.

The main objective of this work is to develop a program to calculate the attenuation of the optical beam between two user-defined points. To do so, we have developed a program in MATLAB that goes through several stages.

First, we process the seabed profile, an important aspect since underwater topography can have a significant effect on light propagation. Next, we calculate the annual mean surface water temperature and the surface chlorophyll concentration using datasets. These data are fundamental to understanding the optical properties of the water in this region. With this information, we can obtain profiles of temperature and chlorophyll concentration at depth, which allows us to model the specific attenuation more accurately at a given point, considering longitude, latitude, depth, and wavelength of the optical beam.

With all these instruments, we can finally calculate the attenuation of the optical beam between two user-specified points. Several factors are considered, such as the distance between points, the chemical composition of the water along the path and the characteristic of the seabed. The result is a reliable programme that allows estimation of optical attenuation in underwater environments, which has an important implication for the development and deployment of underwater communications systems.

1.1 State-of-the-art

About the 70% of the planet's land surface is covered by water. Underwater wireless optical communications are crucial to the development of ocean resources and the protection of the ocean habits [1].

Optical wireless links have found uses in both terrestrial and spaced-based communication systems as well as in atmospheric communication. These links are flexible and can be employed in multiple environments, including both interior and exterior spaces. Additionally, one difficult area in which optical communication has a

demonstrated advantage is underwater environments. In these environments that are submerged, optical wireless communication offers a unique benefit and capacity, this is significant in the exploration of resources and environmental conditions [2].

Underwater optical communications, compared to other types of underwater communications such as acoustic and electronic communications, offers several distinct advantages [3]:

- Speed and bandwidth: Compared to acoustic communications, which have limited bandwidth and slower transmission speeds due to the characteristics of sound waves in water, underwater optical communications can achieve much higher transmission speeds and significantly higher bandwidth. This allows for faster transmission of large amounts of data.
- Security and Privacy: Underwater optical communication offers greater security and privacy compared to electromagnetic communications, which can be susceptible to interception and external interference. Due to the nature of light waves and the lack of electromagnetic radiation, underwater optical communication is more difficult to detect and less prone to external interference, ensuring greater confidentiality in underwater transmissions.
- Energy Efficiency and Compact Size: Underwater Optical Communications requires less energy to operate compared to electromagnetic and acoustic communications. Additionally, the semiconductor light sources used in underwater optical communications have a more compact and lightweight size compared to the transmission and reception equipment of other forms of underwater communication, making it easier to deploy and operate in underwater environments.

Like everything, underwater optical communications have advantages, but they also have disadvantages, such as [3]:

- Development and Implementation Costs: The development of underwater optical communications technologies may require significant investment in research, development, and infrastructure construction. This can increase initial implementation costs.
- Dependence on Light: Underwater optical communications depend on the propagation of light through water. In areas of poor visibility or high turbidity, such as polluted coastlines or oceans, light transmission can be limited, affecting the efficiency of optical communications.
- Susceptibility to Absorption and Scattering: Blue/green wavelengths of light are commonly used in underwater optical communications due to their low attenuation in water but can still suffer from long-range absorption and scattering

problems. This can limit the effective range of underwater optical communications in certain environments.

- Requires precise alignment: Underwater optical communications systems may require precise alignment between transmitters and receivers to maintain optimal connectivity. In dynamic or turbulent underwater environments, this alignment can be difficult to maintain, which can affect the reliability of communications.
- Surveillance Vulnerabilities: Although underwater optical communications offer security and privacy benefits, they can still be vulnerable to surveillance by unauthorized persons. Interception of optical signals underwater can compromise the confidentiality of communication.

In summary, although underwater optical communications have many advantages, they face challenges and limitations that must be addressed to ensure efficiency and reliability in diverse and dynamic underwater environments.

Underwater wireless communications are limited to short distances in the optical frequency range due to strong absorption by water and strong backscattering by suspended particles. However, the underwater EM spectrum has an optical window with relatively low attenuation at blue-green wavelengths. For this reason, underwater optical communications has shown great interest in the development of turquoise sources and detectors. Blue-green wavelengths can demonstrate high bandwidth over medium distances (up to hundreds of meters) [4].

Parameters	Acoustic	RF	Optical
Attenuation	Distance and frequency dependent (0.1 - 4 dB/km) [12]	Frequency and conductivity dependent (3.5 - 5 dB/m) [13]	0.39 dB/m (ocean) - 11 dB/m (turbid) [14]
Speed (m/s)	1500 m/s	$\approx 2.255 \times 10^8$	$\approx 2.255 \times 10^8$
Data rate	~ kbps	~ Mbps	~ Gbps
Latency	High	Moderate	Low
Distance	up to kms	up to ≈ 10 meters	$\approx 10 - 100$ meters
Bandwidth	Distance dependent [8]: 1000 km < 1kHz 1 - 10 km ≈ 10 kHz < 100 m ≈ 100 kHz	\approx MHz	10 - 150 MHz
Frequency band	10 - 15 kHz	30 - 300 Hz (ELF) (for direct underwater communication system) or MHz (for buoyant communication system)	$10^{12} - 10^{15}$ Hz
Transmission power	tens of Watts (typical value)	few mW to hundreds of Watts (distance dependent)	Few Watts
Antenna size	0.1 m	0.5 m	0.1 m
Efficiency	≈ 100 bits/Joules		$\approx 30,000$ bits/Joules
Performance parameters	Temperature, salinity and pressure	Conductivity and permittivity	Absorption, scattering/turbidity, organic matter

Figure 1. Comparison of Different Wireless Underwater Technologies [4]

1. HOW WATER MEDIUM INTERACTS WITH OPTICAL BEAMS

1.1 Specific attenuation

We can define the attenuation as the reduction in the strength of an optical signal, measured in decibels (dB) [5]. Historically, the attenuation coefficient was commonly assumed to remain constant across the entirety of a link. However, research has unveiled the dynamic nature of this coefficient, disproving its steadfastness. Within underwater environments, signal attenuation manifests because of various influencing factors. In this investigation, we aim to address two key factors contributing to optical beam attenuation in the water: light absorption and scattering. To achieve this, we shall formulate an equation for the attenuation coefficient [6]

$$c(\lambda) = a(\lambda) + b(\lambda), \quad (1)$$

where $a(\lambda)$ represents absorption and $b(\lambda)$ represents scattering, and λ is the wavelength of the light transmitting the information. Light absorption can occur due to biological factors, such as phytoplankton, humic acid, fluvic acid, etc. [6] The equation for attenuation can be defined as

$$a(\lambda) = a_w(\lambda) + a_f^0 C_f \exp(-k_f \lambda) + a_h^0 C_h \exp(-k_h \lambda) + a_c^0(\lambda)(C_c/C_c^0)^{0.602}, \quad (2)$$

where $a_w(\lambda)$ is the coefficient of absorption of pure water (m^{-1}) [7], a_f^0 is specific absorption coefficient of fluvic acid ($a_f^0 = 35.959 m^2/mg$), a_h^0 is the specific absorption coefficient of humic acid ($a_h^0 = 18.828 m^2/mg$), a_c^0 is the specific absorption of chlorophyll (m^{-1}). C_c is the concentration of chlorophyll-a (mg/m^3), ($C_c^0 = 1 mg/m^3$); k_f is the fulvic acid exponential coefficient ($k_f = 0.0189 nm^{-1}$) and k_h is the humic acid exponential coefficient ($k_h = 0.01105 nm^{-1}$) [6]. $a_c^0(\lambda)$ is the specific absorption coefficient of chlorophyll

$$a_c^0(\lambda) = A(\lambda)C_c^{-B(\lambda)}, \quad (3)$$

where A and B are constants [8].

C_f is the concentration of fluvic acid (mg / m^3) and C_h is the concentration of humic acid (mg / m^3),

$$C_f = 1.74098 C_c \exp(0.12327 C_c), \quad (4)$$

$$C_h = 0.19334 C_c \exp(0.12343 C_c). \quad (5)$$

In the blue-green sector, pure seawater absorbs minimally but gradually intensifies towards the yellow-red range. In contrast, chlorophyll absorbs most in the blue-green and red segments but least in yellow wavelengths. In clear oceans, pure water absorbs more than chlorophyll due to its lower concentration. However, when chlorophyll concentrations exceed about $2 \text{ mg}/\text{m}^3$, it becomes the primary absorption mechanism, especially for wavelengths below 500 nm.

If focusing on pure water absorption, wavelengths with minimal water absorption, such as those in the blue-green spectrum, are pertinent. Conversely, if investigating chlorophyll's impact, wavelengths where chlorophyll absorption is notable, such as in the blue-green and red regions, are more appropriate [7].

The full equation for the scattering of the water $b(\lambda)$ is given by the relation

$$b(\lambda) = b_w(\lambda) + b_s^0(\lambda)C_s + b_l^0(\lambda)C_l, \quad (6)$$

where $b_w(\lambda)$ is the pure water scattering coefficient (m^{-1}), $b_s^0(\lambda)$ is the scattering coefficient for small particulate matter (m^2/g), b_l^0 is the scattering coefficient for large particulate matter (m^2/g), C_s is the concentration of small particles (g / m^3) and C_l is the concentration of large particles (g / m^3).

$$b_w(\lambda) = 0.005826 \left(\frac{400}{\lambda} \right)^{4.322}, \quad (7)$$

$$b_s^0(\lambda) = 1.1513 \left(\frac{400}{\lambda} \right)^{1.7}, \quad (8)$$

$$b_l^0(\lambda) = 0.3411 \left(\frac{400}{\lambda} \right)^{0.3}, \quad (9)$$

$$C_s = 0.01739 C_c \exp(0.11631 C_c), \quad (10)$$

$$C_l = 0.76284 C_c \exp(0.03092 C_c). \quad (11)$$

Using the provided equations, we can compute the spectral attenuation properties of the water transmission environment for the specified chlorophyll concentrations. This is done by converting the water's extinction coefficient $c(\lambda)$ to the specific attenuation of water α .

1.2 Chlorophyll profile

The foundation of the marine food chain comprises microscopic algae and similar plant like organisms referred to as phytoplankton. Similar to terrestrial plants, phytoplankton employ chlorophyll and other light-absorbing pigments for photosynthesis, converting atmospheric carbon dioxide into sugars for energy. The presence of chlorophyll in water alters its interaction with sunlight, enabling scientists to map the distribution and quantity of phytoplankton. These mappings offer valuable insights into oceanic health and facilitate research on the ocean carbon cycle [9].

Chlorophyll maps illustrate the concentration of chlorophyll per cubic meter of seawater monthly. Regions with minimal chlorophyll content, indicating sparse phytoplankton populations, appear blue. Conversely, dark green hues signify areas abundant in chlorophyll, indicative of robust phytoplankton growth. Data for these observations are sourced from the Moderate Resolution Imaging Spectroradiometer (MODIS) aboard NASA's Aqua satellite. Landmasses are depicted in dark gray, while areas where MODIS data collection was impeded due to factors like sea ice, polar darkness, or cloud cover appear in light gray [9].

The highest concentrations of chlorophyll, where surface-dwelling marine flora thrive, are typically found in cold polar waters or regions influenced by upwelling ocean currents, such as along the equator and coastlines. Cold temperatures often indicate the ascent of nutrient-rich water from deeper ocean layers, fostering phytoplankton growth. Nutrient accumulation during dark winter months in polar waters provides a reservoir for spring and summer blooms when sunlight becomes abundant [9].

A belt of cool, phytoplankton-rich waters encircles the Earth at the Equator, with particularly pronounced effects in the Atlantic and Pacific Oceans. This enhanced phytoplankton growth results from frequent upwelling of deeper, cooler water driven by prevailing easterly trade winds. Along coastal regions, the incline of the seabed promotes upwelling of nutrient-rich water from the ocean depths, facilitating phytoplankton proliferation. Notable instances of this phenomenon occur along the western coasts of North and South America, as well as southern Africa [9].

We can model the chlorophyll concentration profile over depth as a Gaussian curve determined by equation [10]

$$C_c(z) = B_0 + S * z + \frac{h}{\sigma\sqrt{2\pi}} \exp\left[-\frac{(-z - z_{max})^2}{2\sigma^2}\right], \quad (12)$$

where $C_c(z)$ is the chlorophyll concentration (mg/m^3) at depth $z(m)$, B_0 is the background chlorophyll concentration at sea surface (mg/m^3), S is the vertical gradient of the chlorophyll concentration ($mg/m^3/m$), h is the total chlorophyll above the background (mg/m^2), σ , standard deviation of Gaussian distribution, controls the thickness of the chlorophyll maximum layer (m), and z_{max} is the depth of the chlorophyll maximum (m) [10].

$$\sigma = \frac{h}{\sqrt{2\pi}[Chl_{z_{max}} - B_0 - S * z_{max}]}, \quad (13)$$

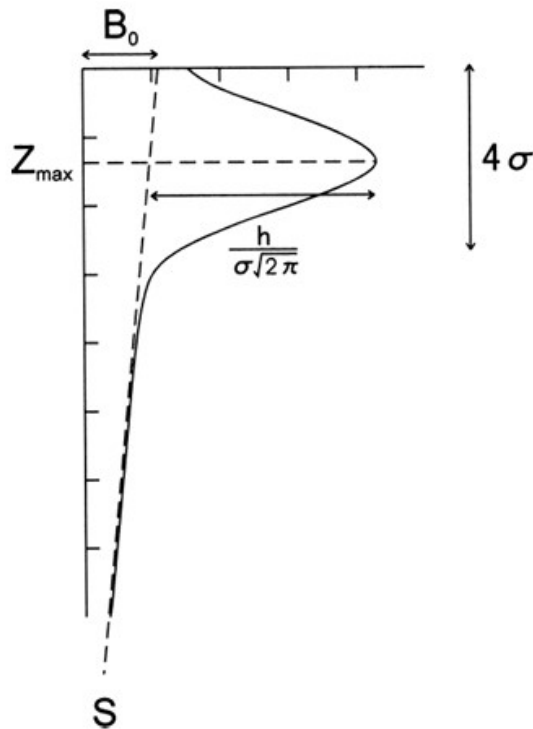


Figure 2: Vertical distribution model of chlorophyll

The vertical distribution of chlorophyll concentration shows regional variability (Matsumura and Shiomoto, 1993; Yokouchi et al., 1996). To address this, the researchers divided the study area into four regions: the Kuroshio region (KR), the warm water region (WM), the cold-water region (CL), and the Oyashio region (OY). Given the temporal and spatial variation of these regions, it is difficult to define their exact geographic boundaries. Earlier studies by Kawai (1972) and Yokouchi et al. (1996) proposed using the temperature exponential to define these limits. The researchers used these exponential temperatures to define the zones as follows: KR: $T(200) \geq 14^{\circ}\text{C}$, OY: $T(100) \leq \text{OY index temperature of OY}$, WM: $T(200) < 14^{\circ}\text{C}$ and $10^{\circ}\text{C} \leq T(100)$ and CL: index temperature of OY $\leq T(100) < 10^{\circ}\text{C}$. where $T(100)$ and $T(200)$ are the water temperature at 100 m and 200 m depth respectively).

Chlorophyll concentrations at the surface ($\text{Chl}_{\text{surface}}$) were categorized into two groups: high concentration ($\text{Chl}_{\text{surface}} \geq 1.0 \text{ mg/m}^3$) and low concentration ($\text{Chl}_{\text{surface}} < 1.0 \text{ mg/m}^3$) [10].

1.3 Temperature profile

To decide the region in which we are, we must know the temperature at a specific point in the ocean at a certain depth. To do this we must know the temperature and depth profile in the ocean.

Typical ocean temperatures range from about -2°C to 30°C . Typically, the warmest ocean waters are near the surface at low latitudes, while the polar ocean waters are much colder. Also, at the same latitude, the waters of the eastern ocean basin are colder than the waters of the western ocean basin. While surface waters are warm, most ocean waters are deeper and colder, with an average ocean temperature of about 4°C [11]. As can be seen in Figure 3, the open sea water temperature distribution in the mid-latitude region shows a typical pattern. Sun-warmed surface waters have high temperatures and low solar penetration, limited to depths less than 1000 m. Because surface water is warmer, it is less dense than deep water, allowing it to retain heat more efficiently. The upper 100-200 m form a mixed layer characterized by a relatively constant temperature. Winds, waves, and ocean currents at the Earth's surface mix the upper layer of water, dissipating heat and maintaining temperature stability in this layer. Below the mixed layer is the thermocline, where the temperature drops rapidly with depth. Beyond the thermocline, the deep ocean extends to the ocean floor and maintains a constant temperature of about 2°C [11]. Maintains a stable environment with small temperature changes. The temperature distribution varies with latitude, with surface waters being colder near the equator and colder at the poles. Tropical regions show a prominent thermocline due to warmer surface temperatures and small seasonal temperature changes. In contrast, the polar regions show little difference between surface and depth temperatures, with consistently cold temperatures and a weak thermocline at all depths. Mid-latitude temperate regions

experience seasonal changes, with surface temperatures varying between 8 and 15°C between summer and winter. As the mixed layer and thermocline deepen, winter storms increase seasonal temperature changes compared to summer. Daily changes in ocean temperature are generally minimal due to the large heat capacity of water [11].

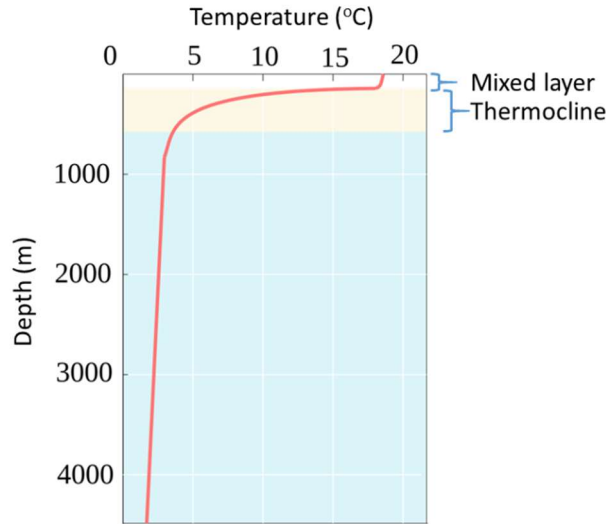


Figure 3. Typical open ocean temperature profile for a mid-latitude region, showing the mixed layer, steep thermocline, and relatively stable temperature at depth.

1.4 Depth dependence

Once the depth chlorophyll profile is quantified, it can be used in conjunction with the chlorophyll attenuation relationship to determine depth-dependent light attenuation. To optimize the scope of the study, the studied communication links work in the open ocean, allowing long-range communication (up to hundreds of meters). In open ocean environments, the lateral deviations of the absorption and scattering coefficients are several kilometres. Therefore, even for long-distance horizontal connections, sea level changes are negligible. This effectively removes the dependency on the (x,y) coordinates of the sea surface.

So, we can rewrite the depth-dependent absorption and scattering equations as

$$a(\lambda, z) = a_w(\lambda) + a_f^0 C_f(z) + a_h^0 C_h(z) \exp(-k_h \lambda) + a_c^0(\lambda) \left(\frac{C_c}{C_c^0} \right)^{0.602}, \quad (14)$$

$$b(\lambda, z) = b_w(\lambda) + b_s^0(\lambda)C_s(z) + b_l^0(\lambda)C_l(z), \quad (15)$$

where now $C_f(z)$, $C_h(z)$, $C_s(z)$ and $C_l(z)$ are the depth dependent profiles of fulvic and humic acid and small and large particles. Recall that the specific attenuation of chlorophyll also contained a chlorophyll concentration term; so now too has depth dependency

$$a_c^0(\lambda, z) = A(\lambda)C_c(z)^{-B(\lambda)}. \quad (16)$$

1.5 Limitations

Due to its development within a MATLAB program, it's reasonable to anticipate that the results of this beam attenuation calculator may not be entirely precise. Several factors contribute to this potential discrepancy in accuracy.

Firstly, the grid spacing of 0.5 between Earth coordinates may result in surface temperature and chlorophyll concentration values with reduced precision. This limitation becomes particularly pronounced when calculating intermediate points between the transmitter and receiver, necessitating approximations of coordinates, which can introduce error into the calculations.

Additionally, the availability of data plays a crucial role. Since coefficient data for all wavelengths is not accessible, the permitted wavelengths are confined to the range of [400-700nm], incremented in steps of 10. This limitation may impact the accuracy of calculations, especially when precise attenuation measurements across various wavelengths are required.

Moreover, it's vital to note that the depth provided must be exact to ensure calculation accuracy. Any deviation in depth values could significantly affect the obtained results.

In summary, while efforts are made to mitigate potential inaccuracies, it's important to consider the inherent limitations when using this beam attenuation calculator. Users should exercise caution when interpreting results and acknowledge the possibility of errors arising from the factors mentioned above.

2. MATLAB PROGRAM

In this part we will explain the code used to calculate the optical beam attenuation. The code can be divided into 7 different parts. The first part covers the processing of the input data needed to perform the following calculations, such as seabed depth [12], water surface temperature [13] and chlorophyll concentration at the water surface [14]. In the second part, the user is asked to enter the points between which the optical attenuation is to be calculated. In the third part, the depth temperature profile of the water medium is calculated. The fourth part is the calculation of the depth concentration of chlorophyll. In the fifth part we will calculate the coordinates of all the points where you are going to calculate the specific attenuation. In the sixth part, with all the previous values calculated, we will calculate the specific attenuation at each point in space. Finally, in the sixth part, we will calculate the optical beam attenuation between the two specified points.

2.1 Input Data

The first part of the code will be used to search and process the datasets needed to perform the calculations. The data values we obtain refer to half-coordinate by half-coordinate data. The code block starts by opening a CSV file containing the seabed profile data, resulting in a 360*720 matrix containing the values of the depth of the ocean. We then create a visual representation to make the map more informative.

In the second part we analyze the temperature at the water surface. For this we read the temperature values of each month from a CSV file and then calculate the average of them, obtaining also a 360*720 matrix with the values of the annual average temperature at the ocean surface with a step of 0.5 coordinates by 0.5 coordinates. In this segment we make an approximation, since being an average of temperatures, there are months in which the results obtained in certain latitudes and longitudes of the ocean are not precise. Since this happens near the poles, we assume that these values are due to the temperature being calculated by reflection in the water, and we set those temperatures to 0°C, since we assume that there is ice or snow in those points during those months.

Finally, in this first part of the code, we will analyze the concentration of chlorophyll on the water surface. We will do this in a very similar way to how we have obtained the surface temperature, since in this part we will also calculate the mean annual chlorophyll concentration, having previously obtained the values of the chlorophyll concentration on the surface of each month and having done the average. We will also make an approximation since when calculating the average, we obtain certain coordinates again in

which in some months the chlorophyll values are not correct, therefore those values are not considered when calculating the average.

2.2 User-specified points

Geographic coordinates are a system used to describe the position of a point on the Earth's surface using two main measurements: latitude and longitude. Latitude refers to the distance measured in degrees from the Equator to the North Pole or South Pole and can range from 0° at the Equator to 90° and -90° at the North and South Poles, respectively. Longitude, on the other hand, refers to the distance measured in degrees from the Greenwich Meridian to the east or west, and can range from 0° to 180° to the east and from 0° to -180° to the west.

In summary, geographic coordinates provide a way to locate any point on the Earth's surface using two angular measurements: latitude and longitude. In this case, latitude values range from -90° to 90° , while longitude values range from -180° to 180° . [15]

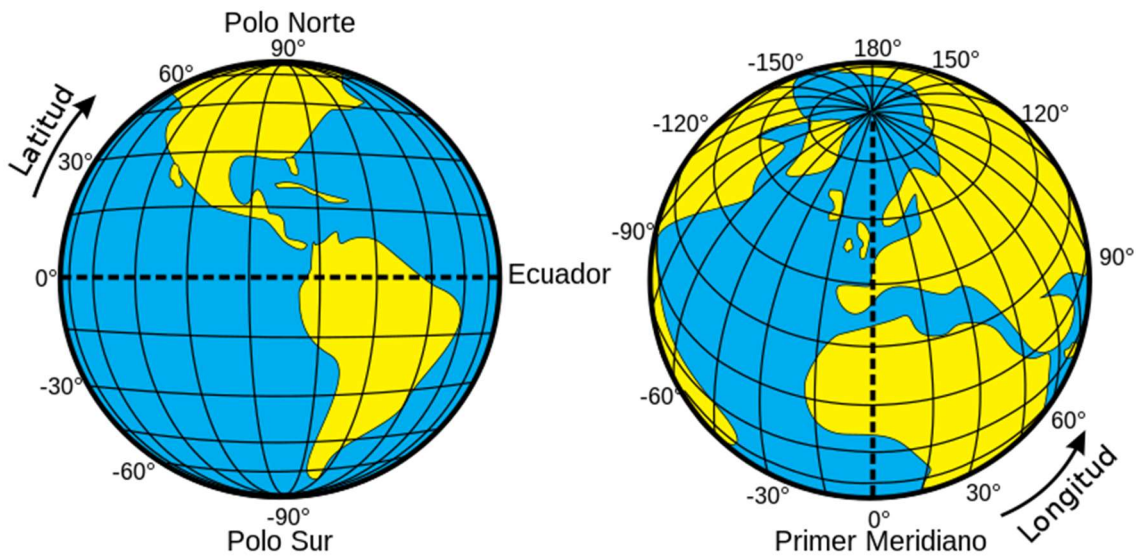


Figure 4. Geographical coordinates

In our application, the user will manually enter geographic coordinates via keyboard input. The acceptable latitude range is -90° to 89.5° with a precision of 0.5° , and the longitude range is -179.5° to 180° with the same precision. These coordinates will be used to retrieve specific data values from pre-stored matrices containing seabed profile, surface temperature, and surface chlorophyll concentration information.

As mentioned earlier, the data is stored in matrices with dimensions of 360 rows (corresponding to latitude values) and 720 columns (corresponding to longitude values).

Therefore, it is necessary to map the user-entered coordinates to the corresponding indices in these matrices to access the desired data points.

We have developed an algorithm that utilizes “if-else” statements to retrieve the desired values. The first step is to verify if the entered coordinates are valid, meaning they fall within the acceptable range. If the coordinates are invalid, an error message will be displayed instructing the user to re-enter the coordinates.

Next, we define the position in our matrices that corresponds to the coordinate (0, 0). In this case, this is set to row 180 and column 360. Subsequently, depending on whether the entered coordinates are positive or negative, different operations are performed to obtain the mapped coordinates.

Once the user-entered coordinates have been validated and confirmed to be within the acceptable range, the algorithm proceeds to access the corresponding data values from the data matrices. This involves retrieving the values for seabed profile, surface temperature, and surface chlorophyll concentration based on the mapped latitude and longitude indices.

This algorithm facilitates the mapping of user-entered latitude and longitude coordinates to corresponding indices in data matrices, enabling the retrieval of specific data values (seabed profile, surface temperature, and surface chlorophyll concentration) for the designated locations. It incorporates input validation, depth validation, and data retrieval steps to ensure the accuracy and reliability of the retrieved information.

```
/*
*****
% Check if the coordinates are within the valid range

if longitud1 >= -90 && latitude 1 <= 89.5 && longitud1 >= -179.5 %%
longitud1 <= 180

% We map the coordinates to obtain the data in the matrix

    if longitud1 >= 0
        longitud_map1 = 360 + (2 * longitud1);
    else
        longitud_map1 = 360 - (2 * abs(longitud1));
    end

    if latitud1 >= 0
        latitud_map1 = 180 - (2 * latitud1);
    else
        latitud_map1 = 180 + (2 * latitud1);
    end
else
    error ('Coordenadas no validas. Vuelve a escribir las coordenadas:
');
end
*/
```

2.3 Depth temperature profile of the water medium

We delineate three distinct zones within the ocean. The first is termed the polar zone, encompassing latitudes between 60°N and 90°N, and 60°S and 90°S. The next zone we designate is the tropical zone, which spans latitudes between 20°S and 20°N. Lastly, we define the mid-latitude zone, which encompasses latitudes between 60°S and 20°S, and 60°N and 20°N.

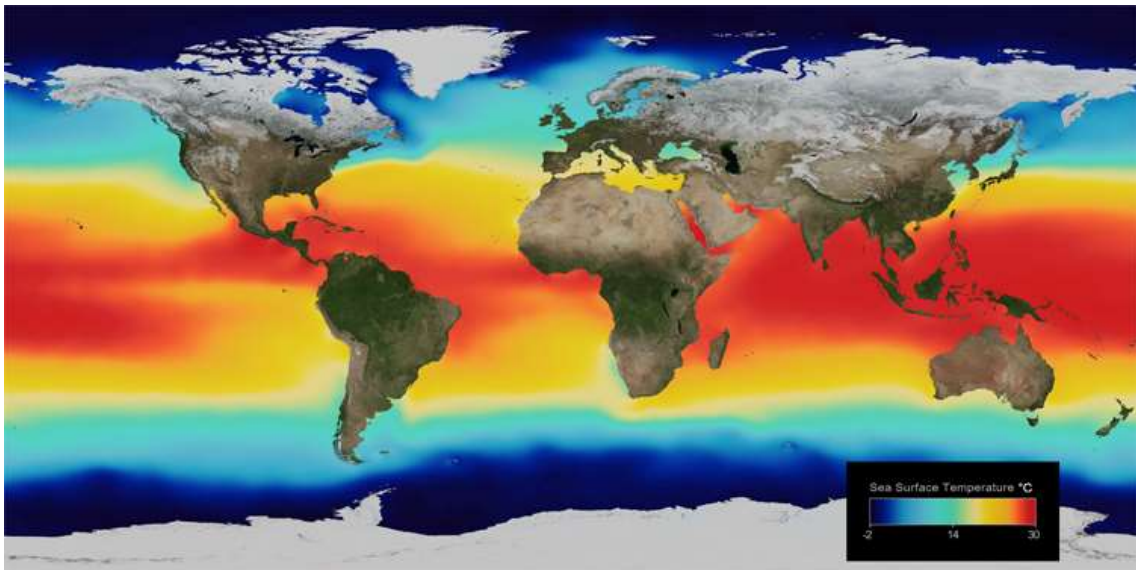


Figure 5. Ocean surface temperature

As we've discussed previously, understanding the ocean's depth involves recognizing its three distinct layers. At the surface lies the surface layer, where the temperature tends to remain relatively constant for the first 200 meters. This stability is largely influenced by factors like wind patterns and wave action, which help maintain uniformity in temperature. As a result, within the initial 200 meters of our depth-temperature profile, we expect to observe temperatures mirroring those found at the surface.

Descending deeper brings us to the abyssal zone, characterized by its profound depths that shield it from external thermal influences. Here, the temperature remains consistent, with specific values assigned to different latitude zones: 1°C for polar regions, 2°C for mid-latitudes, and 4°C for tropical areas. This layer commences at depths exceeding 1000 meters.

Lastly, we encounter the intermediate layer, known as the thermocline, where temperature gradients exhibit a noticeable decline. This transition zone, marked by a rapid decrease in temperature, offers insights into oceanic dynamics. In this layer, the temperature drops

rapidly, and knowing that the temperature is constant both above and below [11][16], it can be calculated as the slope of a line using equation

$$(y - y_1) = m * (x - x_1), \tag{17}$$

where, y is the temperature in the surface, y_1 is the temperature in the abyssal zone, depending on if we are in the polar zone, the tropical zone or the medium-latitude zone, m is the slope of the thermocline, x is the depth where the abisal zone begins (1000m) and x_1 is the depth where the thermocline begins (200m).

Finally, we will plot the temperature values obtained for all the necessary depths using a plot, and we will smooth the graph to give curvature to the intersections between the different layers and make the result as close as possible to the real result.

2.4 Depth concentration of chlorophyll

In this segment of code, our primary objective is to partition the ocean into four distinct zones: KR, OY, WM, and CL [10], each representing a specific geographical area crucial for our analytical framework. To accomplish this division effectively, we rely on boundary conditions derived from temperature data collected at depths of 100 and 200 meters. By scrutinizing these temperature thresholds, we can precisely allocate each geographical point to its corresponding zone.

Once these zones are delineated, our subsequent aim is to establish the necessary parameters for computing the chlorophyll profile equation (12). These parameters serve as the bedrock for characterizing the standard deviation within the Gaussian distribution (13), which in turn allows for the calculation of chlorophyll distribution across the oceanic expanse. It's noteworthy that we tailor these parameters independently for each of the four zones. Depending on the specific zone under examination, we meticulously select parameter values to ensure the accuracy and efficacy of our modelling and analysis endeavours.

This meticulous approach enables us to calibrate our calculations to the distinct environmental characteristics prevalent within each zone, thereby augmenting the precision and applicability of our research findings. By fine-tuning our parameters in accordance with the unique conditions of each zone, we can yield insights that are not only comprehensive but also finely attuned to the intricacies of the oceanic ecosystems in question [10].

2.5 Calculation between the User-specified points

In this part, the first issue we encounter is that when trying to calculate the distance between the two-point positions, we have two different units: the X and Y axes data are in degrees, and the Z-axis data are in meters. To address this, we will convert the X and Y coordinates into distances. We know that 1 degree of latitude on the Earth corresponds to 111.34 kilometres [17].

After standardizing all measurements into a unified unit system, we proceed to compute the distance between the two points using

$$d(P_1, P_2) = \sqrt{(x_1 - x_2)^2 + (y_1 - y_2)^2 + (z_1 - z_2)^2}. \quad (18)$$

where x_1, y_1, z_1 are the longitude, latitude, and depth for the first point, and x_2, y_2, z_2 are the longitude, latitude, and depth for the second point.

Once the distance is established, we subdivide the segment into equidistant intervals to facilitate subsequent calculations of optical attenuation at each interval. In our approach, we opt for a uniform subdivision at intervals of every 1 kilometre. Consequently, it becomes imperative to derive the coordinates for each of these subdivisions

$$P_i = \left(x_1 + \left(\frac{1}{n}\right)(x_2 - x_1), y_1 + \left(\frac{1}{n}\right)(y_2 - y_1), z_1 + \left(\frac{1}{n}\right)(z_2 - z_1)\right), \quad (19)$$

where n represents the total number of intervals into which we partitioned the distance. This meticulous partitioning ensures a granular analysis of the optical properties along the trajectory.

During the computation of coordinates for intermediary points along the segment, it's plausible to encounter coordinate values that do not precisely match our desired format, specifically, they may not terminate precisely at .5 or .0. Consequently, a method for approximating these values is required. To tackle this challenge, we will design a comprehensive algorithm aimed at rounding each coordinate to the nearest appropriate values. This algorithm will ensure that the coordinates maintain consistency and adhere to the desired format for subsequent calculations and analysis.

```

/*****
parte_entera_long = floor(longitudes(o));
parte_decimal_long = longitudes(o) - parte_entera_long;

if parte_decimal_long <= 0.25
    parte_decimal_redondeada_long = 0;
elseif parte_decimal_long <= 0.75
    parte_decimal_redondeada_long = 0.5;
else
    parte_decimal_redondeada_long = 1;
end

longitudes_bien(o) = parte_entera_long + parte_decimal_redondeada_long;

```

In this case, our algorithm deals with the approximation of longitude coordinates, although a similar approach applies to latitude and depth coordinates. The variable "o" serves as an essential component within a looping structure, commonly a "for" loop, utilized to iterate through each calculated point and compute its respective coordinate approximation.

The algorithm initiates by segregating the integer and decimal components of the input number, delineating them into distinct variables for further manipulation. Following this initial step, a series of conditional statements are employed to assess the decimal part's magnitude and ascertain its position within predetermined ranges. These ranges correspond to specific decimal value intervals, dictating the appropriate rounding approach.

Once the appropriate range is identified, the algorithm executes the rounding process, adjusting the decimal part as necessary to ensure conformity with the specified coordinate grid. This meticulous approach guarantees that each coordinate approximation aligns precisely with the desired format, facilitating subsequent analyses and computations.

By meticulously evaluating each decimal component and applying the corresponding rounding operation, our algorithm ensures the accuracy and consistency of the resulting coordinate approximations. This rigorous methodology is essential for maintaining the integrity of subsequent calculations and analyses, ensuring reliable outcomes in applications ranging from geographic mapping to scientific research.

After approximating the coordinates, the next step involves mapping these coordinates, like the procedure outlined in section 2.2. This mapping process allows us to retrieve the depth, temperature, and chlorophyll data for each of the calculated points. By associating the approximated coordinates with corresponding data points, we can effectively analyze and interpret the environmental parameters at various locations within the oceanic region under consideration.

2.6 Calculation of the specific attenuation

The specific attenuation (1) has two distinct components that we need to calculate: absorption (2) and scattering (6). In this section, we will compute these values for the two points entered by the user. Our initial step involves defining all the necessary parameters required for computing these values. This includes factors such as the wavelength of light, depth, temperature, and chlorophyll concentration, among others, which influence both absorption and scattering phenomena in the oceanic environment. Once these parameters are established, we can proceed with the calculations to determine the specific attenuation for the specified points, enabling a comprehensive understanding of the optical properties affecting light transmission in the underwater domain.

In this segment, our task involves accessing a CSV file that houses coefficients corresponding to a variable dependent on the wavelength inputted by the user. Upon accessing this file, we will meticulously compare the user-defined wavelength with the values stored in the CSV. Should a match be found – indicating that the wavelength obtained aligns with a value in the file – we will proceed to define the coefficients A and B using the corresponding values retrieved from the CSV dataset.

Moreover, it's crucial to establish all necessary constants essential for our computational endeavors. These constants play a pivotal role in ensuring the accuracy and reliability of our calculations.

We have to calculate the exact chlorophyll concentration at the user-specified point. This involves meticulous analysis of the previously calculated chlorophyll depth profile, pinpointing the precise value corresponding to the user's chosen depth.

This intricate process highlights the crucial link between chlorophyll concentration and its impact on both absorption and scattering coefficients. Precise determination of this value is paramount, as it directly influences these coefficients, significantly impacting the accuracy of subsequent calculations. Once we have found the absorption and scattering values, we calculate the specific attenuation as the sum of them.

Finally, we need to convert this value, since we want it in logarithmic scale, and it is in linear scale. To do this, we will use (9), where we will define $L = 1$ m since we want the attenuation in dB/m.

2.7 Computing the optical beam attenuation

We can define optical beam attenuation as the sum of specific attenuations multiplied by the distance between the points [18].

While the previous computations have provided valuable insights, they were limited to the specific points designated by the user and the intermediate points calculated in between. To determine the total beam optical attenuation, we must extend our analysis to

encompass each one of these points. This necessitates the calculation of the specific attenuation at every single location and subsequent summation of these individual values. Therefore, the final stage of our algorithm can be effectively implemented as a loop. This loop iterates through the previously calculated approximate longitudes, latitudes, and depths, encompassing the entire user-defined area. At each of these points, we meticulously calculate the depth temperature profile and the depth concentration of chlorophyll. These values are then utilized to determine the specific attenuation, which is meticulously stored in a designated variable.

Once the specific attenuation has been calculated at each point, since we have divided the segment into equal parts, we know that all the points are 1000m apart (a value that we defined previously), except for the initial and final points, which would be 500m apart. The result will be a result of in dB.

3. RESULTS

The first thing we must do is select two points between which we can calculate the attenuation. For this, the program shows us a world map so that we can select the correct coordinates.

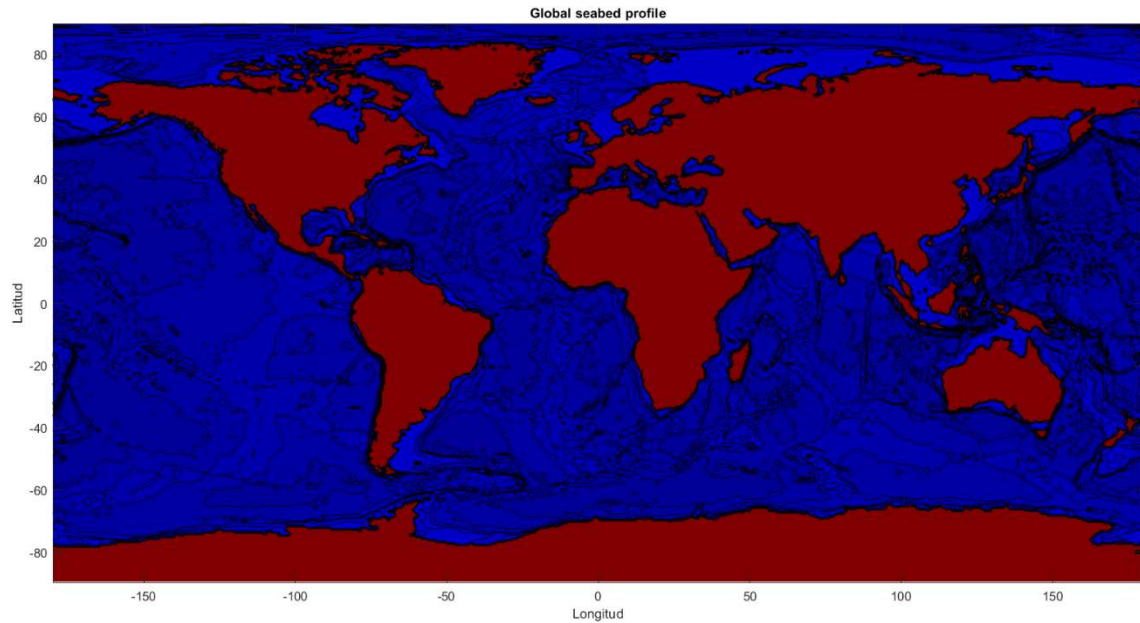


Figure 6: Global seabed profile.

The program also displays a map showing chlorophyll concentration and sea surface temperatures.

The program prompts us to enter the coordinates manually using the keyboard.

```
Introduzca la longitud del primer punto (x) (-179.5 a 180): -120
Introduzca la latitud del primer punto (y) (-90 a 89.5): 0
Introduzca la longitud del segundo punto (x) (-179.5 a 180): -120
Introduzca la latitud del segundo punto (y) (-90 a 89.5): 0
```

Figure 7

For our example, we have chosen the coordinates (-120, 0) for the first point and (-120, 0) for the second point.

The same applies to both the wavelength and the depth of the points. In this case, we have chosen a wavelength of 460nm, which is within the range of visible wavelengths. In this case, it would correspond to blue [15], and depths of 200 and 230 meters for the first point and the second point, respectively.

```
Wavelength (400-700 nm): 460  
Depth of point one: 200  
Depth of point two: 230
```

Figure 8

Once the coordinates are mapped, we obtain the values for depth, surface temperature, and chlorophyll concentration. As we can see, these values are very similar since we have chosen close points.

- Depth

```
profundidad1 = -4.1890e+03  
profundidad2 = -4.1890e+03
```

Figure 9

- Surface Temperature and chlorophyll concentration in first point

```
C_sup1 = 0.1615  
T_sup1 = 26.8058
```

Figure 10

- Surface Temperature and chlorophyll concentration in second point

```
C_sup2 = 0.1615  
T_sup2 = 26.8058
```

Figure 11

Once these values have been calculated, we proceed to calculate the depth temperature profile for these two points. As we can tell from the latitude, the points are located in the tropical zone.

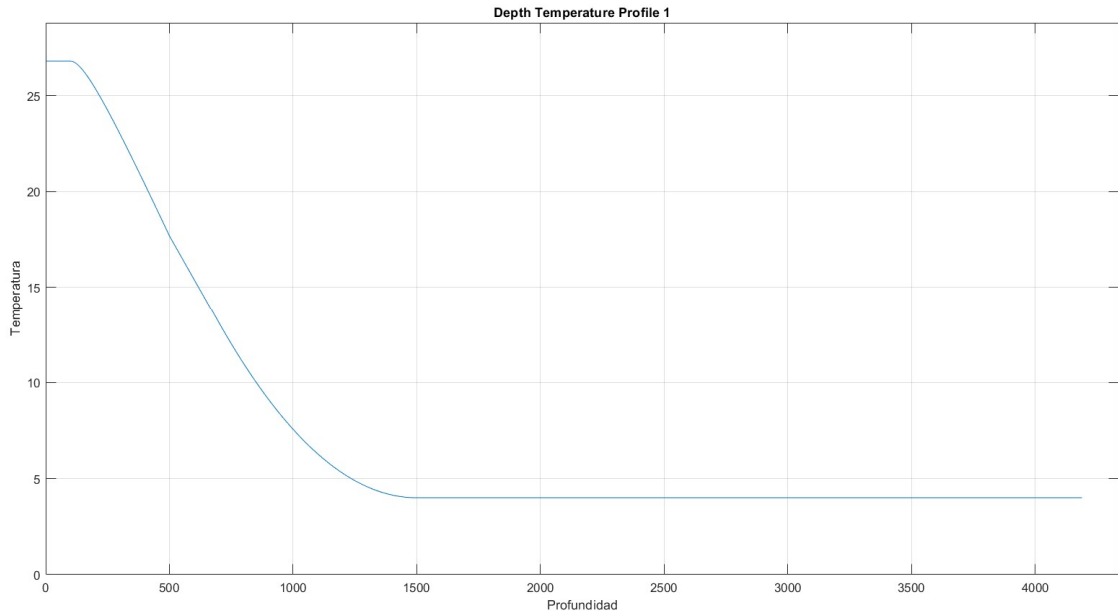


Figure 12: Depth temperature profile for point 1.

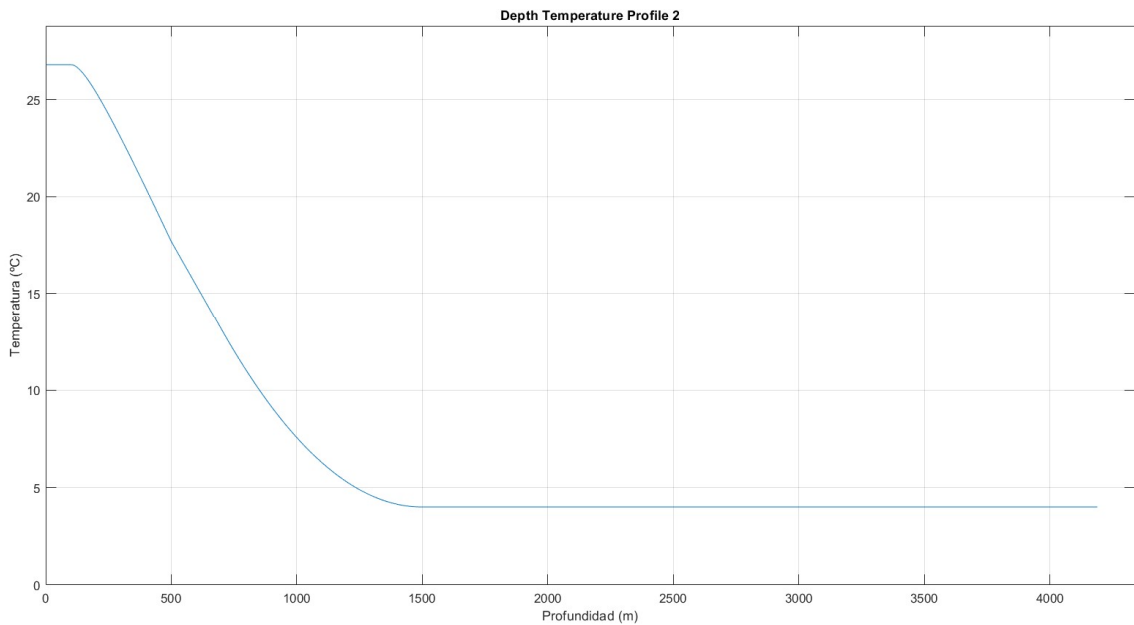


Figure 13. Depth temperature profile for point 2.

The examination of water temperature profiles generated in MATLAB unveils striking resemblances to real profiles encountered in natural aquatic environments. This profile offers a nuanced insight into ocean temperature distribution, showcasing three discernible zones within the water column.

The initial and final regions exhibit notable stability within this range, indicating a relatively uniform temperature regime in these areas. Conversely, the middle zone, commonly termed the thermocline, displays a distinctive temperature pattern that declines rapidly with increasing depth. This phenomenon mirrors the dynamic nature of oceanic thermal stratification, where different layers of the water column exhibit varying thermal properties.

Adapting these MATLAB-derived profiles to real-world conditions yields valuable insights into the complex interplay between ocean dynamics and temperature distribution, aiding in a better understanding of aquatic ecosystems and environmental processes.

Next, we will generate the depth concentration chlorophyll profiles. Firstly, it is essential to ascertain the specific zone among the four defined ones based on the temperature readings at various points. This initial step is crucial as it sets the stage for subsequent calculations and analysis. Once the zone classification is completed, we can delve into the calculation of the chlorophyll concentration profile. This involves meticulous computations and data processing to derive accurate representations of chlorophyll distribution across different depths.

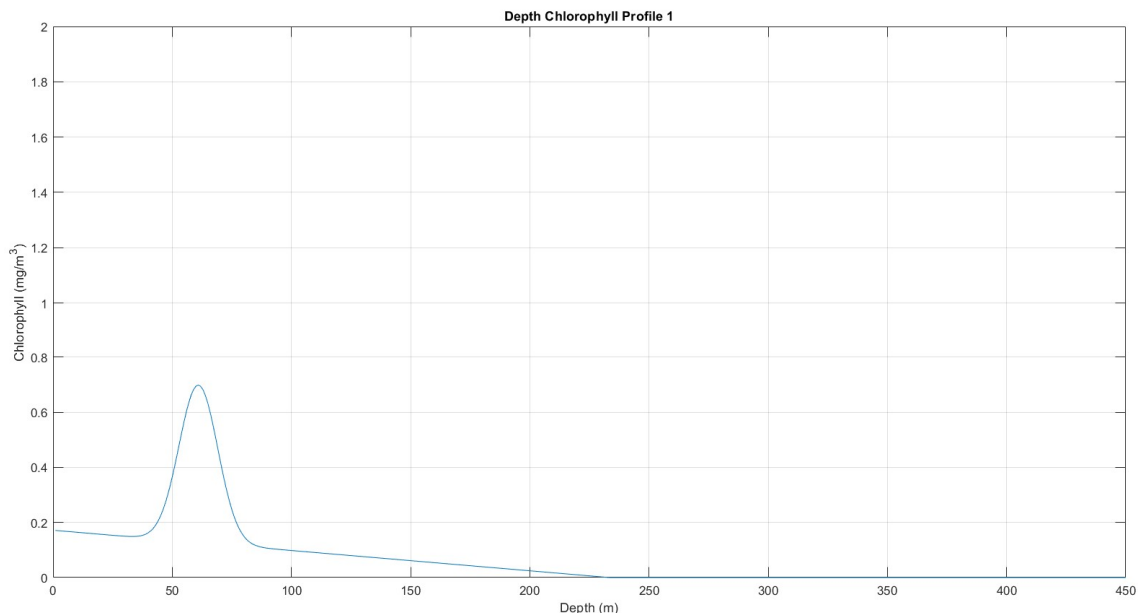


Figure 14: Depth Chlorophyll Profile of point 1.

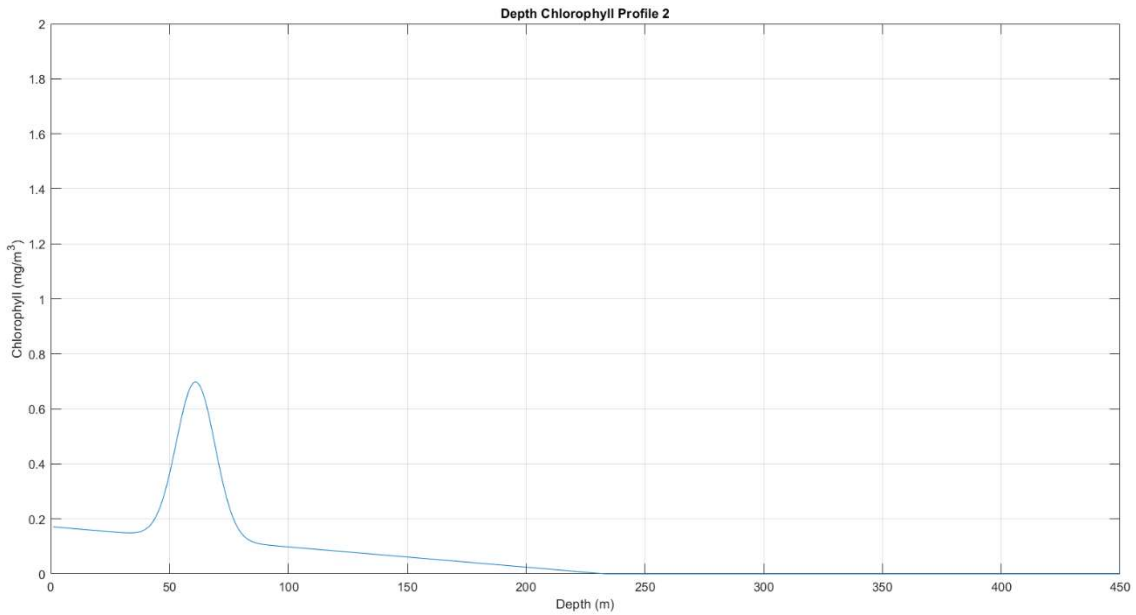


Figure 15: Depth Chlorophyll Profile of point 2.

It becomes evident that the resulting values closely align with a Gaussian function. This correspondence between the observed data and the Gaussian function is noteworthy, as it signifies a coherent relationship between the empirical findings and theoretical expectations. Such congruence lends credence to the validity of the methodology employed and the accuracy of the measurements obtained.

In conclusion, the successful derivation of the chlorophyll concentration profile, characterized by its resemblance to a Gaussian function, underscores the effectiveness of the analytical approach adopted in this study.

Now, we proceed to calculate the distance between the two points:

$$\text{distance} = 30$$

Figure 16

The distance is in meters.

As previously stated, since we decided to define points every 10 meters, we obtain a total of 3 points in which we calculate the specific attenuation.

As we approach the conclusion of our process, the penultimate step entails determining the specific attenuation at the designated points along our path. To achieve this, we begin by obtaining the values in their linear form, ensuring a comprehensive understanding of the signal's behavior as it traverses through the underwater medium. This initial

transformation lays the groundwork for further analysis, enabling us to delve deeper into the intricate dynamics of signal attenuation and its implications for underwater communication systems.

```
specific_attenuation1 = 1.7574  
specific_attenuation2 = 0.3927
```

Figure 17

The attenuation is calculated in decibels (dB) because it provides a convenient way to express the relationship between two power levels. In the context of optical signal transmission, such as in underwater communication, attenuation refers to the reduction of signal power as it travels through the medium, in this case, water. Expressing attenuation in dB allows for a logarithmic representation of this reduction, facilitating comparison between different attenuation levels and understanding signal loss based on distance or medium conditions.

```
specific_attenuation1_dB = -7.6322  
specific_attenuation2_dB = -1.7055
```

Figure 18

The final step in our process involves calculating the specific attenuation at each of the points we have previously determined, and then summing these values together to derive the total attenuation. This comprehensive assessment of attenuation across the entire distance between the two points provides us with a thorough understanding of how optical signals are affected as they propagate through the underwater environment. By analyzing the attenuation at each point along the path, we can gain insights into the cumulative impact of various factors such as water turbidity, chlorophyll concentration, and other environmental variables on the integrity of the optical signal. This information is crucial for designing effective communication systems and optimizing their performance in underwater settings.

```
ALPHA_TOTAL = -117.0125
```

Figure 19

4. CONCLUSION

As we can see in the simulation result, the total attenuation of the link is -117.0125 dB. Following the formula [19],

$$\text{dB} = 10 \log_{10} \left(\frac{P_o}{P_i} \right) \quad (20)$$

where P_o represents the output power and P_i denotes the input power. A reduction of -3 dB indicates a halving of the signal power. With a link spanning 30 meters, we can ascertain an attenuation rate of approximately -3.9 dB/m.

While the measured attenuation coefficient of -3.9 dB/m may initially appear high, it is important to consider the unique context of this study: a wireless optical communication operating underwater, a different scenario from traditional cable transmission.

Therefore, when we observe higher attenuation levels in the ocean, it likely indicates an increased presence of chlorophyll at specific depths. This correlation between measured attenuation and chlorophyll concentration underscores the intricate link between biological processes and the optical properties of a aquatic ecosystems. Notably, a typical attenuation value in turbid water is around 11 dB/m [4], a slightly higher value than ours, (as we have discussed earlier, a -3dB figure halves the signal, while a 3dB figure doubles the power). This alignment suggests that our simulation results fall within a reasonable range, further supporting their accuracy.

LITERATURE

- [1] Sun, C., Wang, W., & Lin, C. (2023). *Special issue "underwater wireless optical communication, sensor and network"* https://www.researchgate.net/publication/374476456_Special_Issue_Underwater_Wireless_Optical_Communication_Sensor_and_Network
- [2] Hudcova, L., & Wilfert, O. (2021). Calculation of the applicable wavelengths in underwater communication. Paper presented at the pp. 1-5. doi:10.1109/COMITE52242.2021.9419881
- [3] Huang, X., & Yang, F. (2019). Hybrid LD and LED-based underwater optical communication: State-of-the-art, opportunities, challenges, and trends [invited]. *Chinese Optics Letters*, 17, 100002. doi:10.3788/COL201917.100002
- [4] Ledig, C., Theis, L., Huszar, F., Caballero, J., Cunningham, A., & Acosta, A. (2017). Href {<https://ieeexplore.ieee.org/abstract/document/8099502>} {photo-realistic single image super-resolution using a generative adversarial network}. Paper presented at the *Cvpr*, 2. (3) pp. 4.
- [5] Lara. (2023, 14 enero). *Atenuación y pérdida en la fibra óptica*. FibraMarket la Fibra Optica de Mexico. <https://www.fibramarket.com/atenuacion-y-perdida-en-la-fibra-optica>
- [6] Johnson, L., Green, R. J., & Leeson, M. (2013). Underwater optical wireless communications: Depth dependent variations in attenuation. *Applied Optics*, 52, 7867-73. doi:10.1364/AO.52.007867
- [7] *Optica Publishing Group*. (s. f.). <https://opg.optica.org/ao/fulltext.cfm?uri=ao-36-33-8710&id=63107>
- [8] Bricaud, A., Babin, M., Morel, A., & Claustre, H. (1995). Variability in the chlorophyll-specific absorption coefficients of natural phytoplankton: Analysis and parametrization. *Journal of Geophysical Research*, 100, 13,321-13,332. doi:10.1029/95JC00463
- [9] NASA Earth Observatory. (s. f.). *Chlorophyll*. https://earthobservatory.nasa.gov/global-maps/MY1DMM_CHLORA#:~:text=The%20highest%20chlorophyll%20concentrations%2C%20where,along%20the%20shores%20of%20continents.
- [10] Kameda, T., & Matsumura, S. (1998). Chlorophyll biomass off sanriku, northwestern pacific, estimated by ocean color and temperature scanner (OCTS) and a vertical distribution model. *Journal of Oceanography*, 54, 509-516. doi:10.1007/BF02742452
- [11] Webb, P. (s. f.). 6.2 *temperature*. Pressbooks. <https://rwu.pressbooks.pub/webboceanography/chapter/6-2-temperature/>

- [12] NASA EARTH OBSERVATION (2024) Chlorophyll Concentration (1 month aqua/modis) https://neo.gsfc.nasa.gov/view.php?datasetId=MY1DMM_CHLORA
- [13] NASA Earth Observations (NEO). (s. f.). Bathymetry (GEBCO) | NASA. Bathymetry (GEBCO) | NASA. https://neo.gsfc.nasa.gov/view.php?datasetId=GEBCO_BATHY
- [14] NASA Earth Observations (NEO). (s. f.-b). Sea Surface Temperature (1 month - Aqua/MODIS) | NASA. Sea Surface Temperature (1 Month - Aqua/MODIS) | NASA. <https://neo.gsfc.nasa.gov/view.php?datasetId=MYD28M>
- [15] Ibañez Asensio, S., Gisbert Blanquer, J. M., & Moreno Ramón, H. (2010). Coordenadas geográficas <https://riunet.upv.es/bitstream/handle/10251/8931/Coordenadas%20geogr%C3%A1ficas.pdf>
- [16] Fundación Aquae. (2021, 20 octubre). Zonas del océano: densidad y profundidad - Fundación Aquae. <https://www.fundacionaquae.org/wiki/las-diferentes-zonas-de-los-oceanos-por-densidad-y-por-profundidad/>
- [17] Navarro, M. Á. M. (s. f.). Longitud y latitud. https://manualvuelo.es/7navg/72_scord.html#:~:text=Un%20grado%20de%20latitud%20corresponde,equivalente%20a%20111%2C32%20Km.%20https://rcti.com.mx/index.php/blog/item/60-atenuacion-fo
- [18] Carrillo Lopez. D. Colores espectrales <https://www-elec.inaoep.mx/~rogerio/Colores%20espectrales.pdf>
- [19] Perez P.F ¿Qué es el dB? Facultad Regional Mendoza <http://www1.frm.utn.edu.ar/medidase2/varios/dB.pdf>